[15]E. M. Riordan *et al.*, Phys. Rev. Lett. 33, 561 (1974); R. E. Taylor, in *Proceedings of the International Symposium on Lepton and Photon Interactions at High Energies, Stanford, California, 1975*, edited by W. T. Kirk (SLAC, Stanford, Calif., 1975); W. B. Atwood, SLAC Report No. 185, 1975 (unpublished).

Production of Muon Pairs by 225-GeV/c $\pi^\pm$, K^+, $p^\pm$ Beams on Nuclear Targets

K. J. Anderson, R. N. Coleman,[a] G. E. Hogan, K. P. Karhi, K. T. McDonald, C. B. Newman, J. E. Pilcher, E. I. Rosenberg, G. H. Sanders,[b] A. J. S. Smith, and J. J. Thaler

Enrico Fermi Institute, University of Chicago, Chicago, Illinois 60637, and University of Illinois, Urbana, Illinois 61801, and Joseph Henry Laboratories, Princeton University, Princeton, New Jersey 08540

(Received 22 January 1979)

Results are presented from a large-acceptance experiment in which muon-pair production was observed in the mass range 2 to 11 GeV/c^2. Data were taken with $\pi^\pm$, K^+, and $p^\pm$ beams at 225 GeV/c on carbon, copper, and tungsten targets. Differential cross sections and the production dependence on pair mass, x_F, p_T, incident-particle type, and target nucleus are discussed.

Lepton-pair production in hadron interactions has been a particularly fruitful area for testing current ideas on hadronic structure. In this Letter we report the most recent of a series of measurements on μ-pair production. The data have more than a factor of 50 greater sensitivity than our previous measurements[1] and explore several features of the production which have not been studied before.

The measurements were carried out with the Chicago cyclotron magnet spectrometer in the Muon Laboratory at Fermilab. The basic configuration of the spectrometer is discussed in our previous work.[1] The major modifications for this experiment consisted of, (1) installation of larger multiwire proportional chambers upstream of the cyclotron magnet to increase acceptance at low Feynman x (x_F) and high pair mass, (2) addition of a second large hodoscope array downstream of the magnet, and (3) addition of mass-threshold logic to the trigger to permit the use of higher-intensity incident beams. Details of the trigger, mass-threshold logic, and the spectrometer are presented elsewhere.[2] Improvements in the beam-line configuration resulted in an order-of-magnitude increase in available beam intensities.

An unseparated positive or negative beam of 225-GeV/c hadrons ($\pi^\pm, K^\pm, p^\pm$) was focused to a 2-cm × 3-cm spot at the experimental target. Four threshold gas Cherenkov counters were placed in the beam to identify the particle type. For negative running, all counters were set just below $\bar{p}$ threshold. For positive beams, two counters were set below K threshold and two were set below proton threshold. The pion component of the positive beam was enhanced at the expense of total transmission, by placing a polyethylene absorber in the beam about 300 m upstreat of the spectrometer. With this absorber pions constituted 28% of the positive flux. The resulting positive beam intensity was kept below 10^7/sec to allow π-K-p separation. Negative intensities of up to 2×10^7/sec were obtained.

Carbon, copper, and tungsten targets, each 1 absorption length thick, were used. The carbon target was divided into three segments of equal thickness, separated by scintillation counters. The scintillator pulse heights were used to localize the beam interaction point and hence to test for thick-target effects. Production of μ pairs by secondary particle interactions in the target would appear as an excess of counts at low Feynman x ($x_F = P_L^*/P_{max}^*$) for the events originating in the downstream target segment. A comparison of x_F distribution of 10 000 J/ψ events originating in the upstream and downstream target segments reveals no evidence of secondary interactions.

For reasons described in the following paper,[3] a carbon target was used to measure μ-pair production cross sections from π^+ and π^- beams. Special care was taken to maintain similar operating conditions for the two beam polarities. Following this phase of running, Cu and W targets were used with the highest available negative-beam rates.

The event reconstruction is very similar to that of our previous experiment which has already

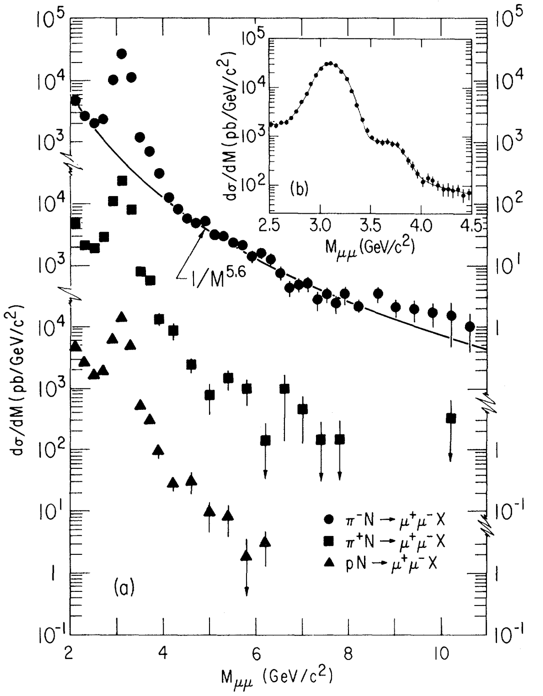

FIG. 1. (a) Differential cross section per nucleon vs mass for π^-, π^+, and proton beams. (b) Differential cross section per nucleon vs mass for $2.0 < M < 4.5$ GeV/c^2, $\pi^- N \rightarrow \mu^+\mu^- X$. The solid line is the sum of the Monte Carlo–calculated J/ψ and ψ' line shapes with an exponentially decreasing continuum.

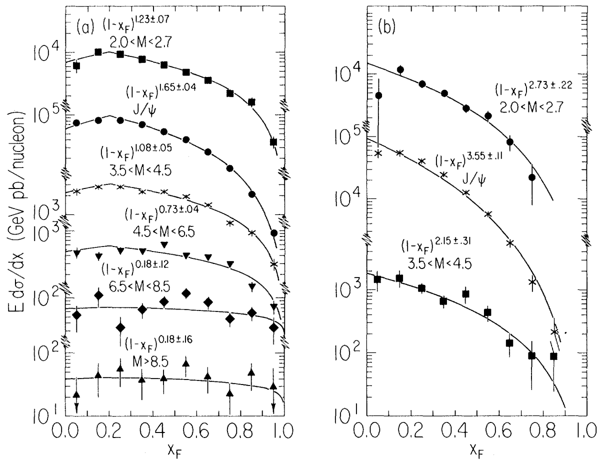

FIG. 2. $E d\sigma / d x_F$ vs x_F for various mass intervals. (a) $\pi^- N \rightarrow \mu^+\mu^- X$, (b) $pN \rightarrow \mu^+\mu^- X$. The solid curves show fits to the region $0.2 < x_F < 1$. The fits have been reflected about $x_F = 0.2$ to compare with the two data points below 0.2. The justification for assuming a maximum in these distributions away from $x_F = 0$ follows from Ref. 7 which observed production in both the forward and backward hemispheres at comparable c.m. energy.

been described.[4] The muon tracks were required to form a vertex in the target within resolution and to strike hodoscope counters which satisfied the trigger logic requirements. The reconstruction efficiency as determined by visual scanning of computer-displayed events was 0.92 ± 0.04.

The spectrometer has large acceptance in μ-pair mass, x_F, p_T, and pair decay angle. Since the distributions in all production variables are directly measured, no assumptions are needed to determine the μ-pair cross sections. The x_F acceptance covers the full forward hemisphere for all masses considered and ranges from approximately 6% at $x_F = 0$ to 30% at $x_F = 0.8$.

Figure 1(a) shows the mass spectra measured for π^-, π^+, and p beams. The systematic uncertainty of 15% is not included in the error bars of Figs. 1 or 2. The systematic effects arise from uncertainties in acceptance, absolute normalization, and atomic-number dependence of the cross section. Other contributions have been investigated but are small on this scale. The A dependence used in determining cross sections per nucleon is measured in this experiment and is discussed below. We consider first the features of resonance production.

The distributions are dominated by the J/ψ signal. The J/ψ cross sections from the carbon target are listed in Table I for $x_F > 0$. These values are expected to be more reliable than those we have reported previously[1] since no fit to the data is required to estimate the cross section near $x_F = 0$. K^+- and $\bar{p}$-induced J/ψ events were also observed and production cross sections are included in Table I. K^+ and $\bar{p}$ normalization uncertainties dominate the quoted errors.

The $\psi'(3.7)$ signal is observed in the π^--, π^+-, and proton-beam data samples and is shown for

TABLE I. J/ψ and $\psi'(3.7)$ cross sections on carbon target ($x_F > 0$). Systematic errors have been included and dominate the quoted error.

Beam	$B\sigma(J/\psi)$ (nb/nucleus)	$B\sigma(\psi')/B\sigma(J/\psi)$
π^-	88 ± 12	0.021 ± 0.006
π^+	82 ± 12	0.017 ± 0.009
p	53 ± 7	0.016 ± 0.009
K^+	49 ± 15	...
$\bar{p}$	85 ± 40	...

the π^- data in Fig. 1(b). The cross section times branching fraction for $\psi'(3.7)$ production relative to J/ψ is included in Table I.

No conclusive evidence is seen for an enhancement at 9.5 GeV/c^2. The mass resolution of the apparatus at 9.5 GeV is determined to be $\sigma_M = 380$ MeV/c^2 by a Monte Carlo calculation which faithfully reproduces the observed J/ψ and ψ' linewidths as shown in Fig. 1(b). At the 95% confidence level we set a limit of $B\sigma_\Upsilon = 1.4$ pb/nucleon for incident π^- at 225 GeV/c. The sensitivity of this result can be compared to the reported limit on proton-induced upsilons at 200 GeV/c. In a 1.0-GeV/c^2-wide mass region, we find $B\sigma_\Upsilon$/continuum $= 0.4 \pm 0.4$ while Yoh *et al.*[5] report 0.1 $\pm$ 0.1.

Continuum pairs in the π^--induced data are observed out to ~11 GeV/c^2 in mass. The shape of the continuum in the region 2–8 GeV/c^2 is reasonably represented by $d\sigma/dM \propto M^{-5.6 \pm 0.05}$. The π^+- and proton-induced distributions fall off more rapidly with increasing pair mass as can be seen from Fig. 1(a).

The cross section $Ed\sigma/dx_F$ from π^--induced pairs is shown in Fig. 2(a) for several mass intervals from 2.0 to 11 GeV/c^2.[6] The x_F spectrum for J/ψ production is distinctly steeper than is observed for the mass continuum regions above and below the resonance. Another important feature of these distributions is that as the pair mass increases the x_F spectrum becomes progressively flatter. Similar features are observed in the proton-induced data shown in Fig. 2(b).

In Fig. 3(a), the mean transverse momenta for π^--induced events with $x_F > 0$ are plotted versus pair mass. Data from other measurements are shown for comparison. The mean p_T increases with mass up to $M \sim 4$ GeV/c^2, where it reaches a plateau value of approximately 1.2 GeV/c. A similar plateau is seen for the proton-induced data of Yoh *et al.*,[5] but a value 200 MeV/c lower.

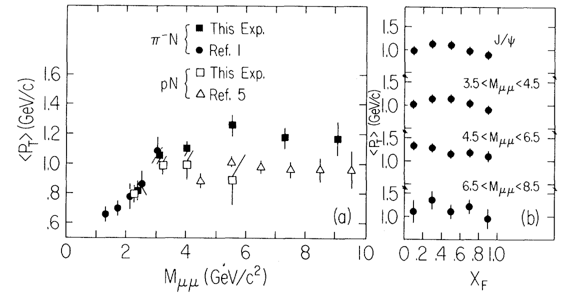

FIG. 3. (a) Mean transverse momentum vs mass for $(\pi^-/p)N \to \mu^+\mu^- x$. (b) Mean transverse momentum vs x_F for $\pi^- N \to \mu^+\mu^- X$.

Proton-induced data from our experiment also exhibit a lower $\langle p_T \rangle$ at $M \sim 4$ GeV/c. These results are summarized in Table II, together with measurements of $\langle p_T^2 \rangle$ for the various beam-particle types and mass intervals. The dependence of $\langle p_T \rangle$ on x_F is displayed in Fig. 3(b) for several intervals of pair mass. Within uncertainties of ~100 MeV/c, no variation of $\langle p_T \rangle$ with x_F is observed.

Previous measurements[1,8-10] have shown that the cross sections for μ-pair production from different nuclei vary as $\sigma_0 A^\alpha$, where A is the atomic mass number of the target material, σ_0 is the free-nucleon cross section, and α is a constant which may depend on the kinematic region under consideration. The π^--induced data from C, Cu, and W targets were divided into a number of kinematic intervals in order to determine α and its variation. The statistical error for each cross section was combined with a 12% systematic uncertainty. In each interval the data were well represented by the power-law dependence. The variation of α with kinematic region is shown in Fig. 4. Figure 4(a) shows a systematic increase of α with p_T in the J/ψ interval. Similar results have been reported for other in-

TABLE II. Mean transverse momentum and mean transverse momentum squared versus muon-pair mass and beam-particle type.

Mass (GeV/c^2)	$\langle p_T \rangle$ (GeV/c) p	$\bar{p}$	π^+	π^-	$\langle p_T^2 \rangle$ (GeV^2/c^2) p	$\bar{p}$	π^+	π^-
2.0–2.7	0.79±0.10	1.17±0.34	0.82±0.10	0.82±0.10	0.81±0.10	1.80±0.50	0.87±0.10	0.89±0.10
J/ψ	0.97±0.10	0.88±0.13	1.01±0.10	1.05±0.10	1.25±0.10	1.02±0.14	1.33±0.10	1.47±0.10
3.5–4.5	1.00±0.13	1.26±0.49	1.05±0.12	1.10±0.10	1.42±0.15	1.70±0.70	1.47±0.14	1.64±0.10
4.5–6.5	0.87±0.21	⋯	1.16±0.25	1.25±0.10	0.91±0.20	⋯	1.63±0.34	2.06±0.11
6.5–8.5	⋯	⋯	1.08±0.45	1.17±0.12	⋯	⋯	1.56±0.65	1.79±0.15
8.5–12.0	⋯	⋯	⋯	1.17±0.16	⋯	⋯	⋯	1.57±0.20

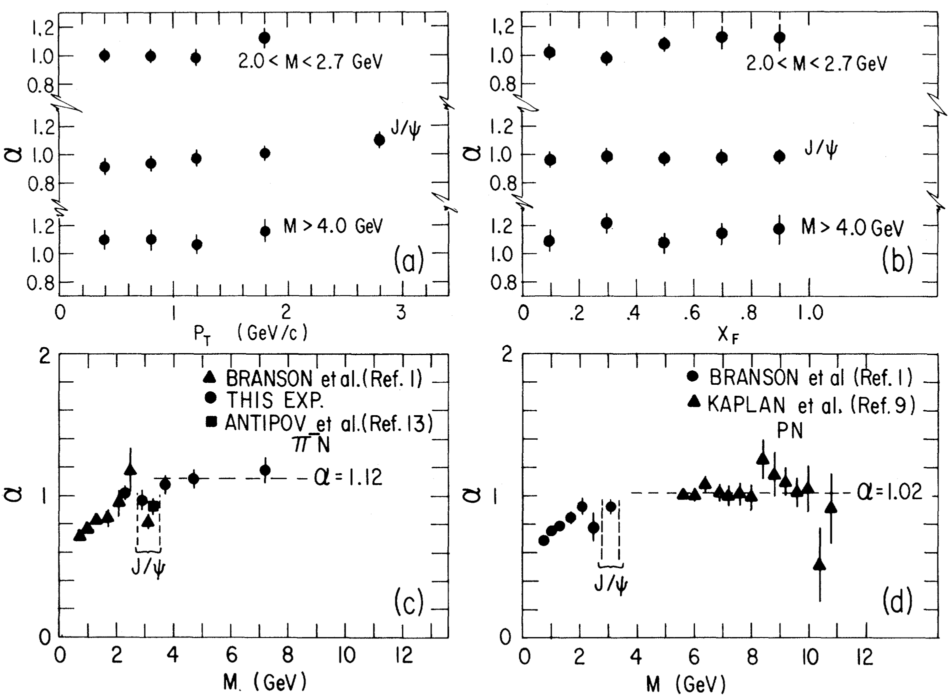

FIG. 4. The atomic mass number dependence A^{α} is displayed for $\pi^- N \rightarrow \mu^+\mu^- X$. (a) α vs transverse momentum of the muon pair. (b) α vs x_F. (c) α vs M. (d) α vs M for $pN \rightarrow \mu^+\mu^- X$.

clusive hadron production[11] and have prompted considerable theoretical discussion.[12] Figure 4(b) shows no significant variation of α with x_F. The mass dependence of α integrated over p_T and x_F is shown in Fig. 4(c). Included in the figure are previous measurements at lower mass. The data show a rise of α with increasing μ-pair mass in the region below the J/ψ. A plateau in α is reached at higher mass values and the mean value for $M > 4$ GeV is $\alpha = 1.12 \pm 0.05$. This is the value used for the data of Fig. 1, except for the J/ψ where $\alpha = 0.87$ was used. A similar plateau in α has been observed in proton-induced data shown for comparison in Fig. 4(d), although there the plateau value is 1.02.[9]

The data presented in this paper have important implications for the quark-antiquark annihilation picture. These implications are discussed in subsequent Letters.[3,14]

This work was performed at the Fermi National Accelerator Laboratory and supported by the U. S. Department of Energy and the National Science Foundation.

(a) Present address: University of Rochester, Rochester, N. Y. 14627.

(b) Present address: Los Alamos Scientific Laboratory, Los Alamos, N. M. 87545.

[1] J. G. Branson *et al.*, Phys. Rev. Lett. 38, 1334 (1977), and references contained therein.

[2] G. E. Hogan, to be published.

[3] G. E. Hogan *et al.*, following Letter [Phys. Rev. Lett. 42, 948 (1979)].

[4] K. J. Anderson *et al.*, to be published; J. G. Branson, Ph.D. thesis, Princeton University, 1977 (unpublished).

[5] J. K. Yoh *et al.*, Phys. Rev. Lett. 41, 684 (1978).

[6] The definition of x_F used in Fig. 3 takes into account the finite mass of the muon pair. At $M_{\mu\mu} = 8.5$ GeV/c^2, for example, $x_F = 2P_L^*/0.83\sqrt{s}$.

[7] M. A. Abolins *et al.*, in Proceedings of the Nineteenth International Conference on High Energy Physics, Tokyo, Japan, 1978 (to be published).

[8] M. Binkley *et al.*, Phys. Rev. Lett. 37, 571 (1976).

[9] D. M. Kaplan *et al.*, Phys. Rev. Lett. 40, 435 (1978); L. M. Lederman, in Proceedings of the Nineteenth International Conference on High Energy Physics, Tokyo, Japan, 1978 (to be published).

[10] D. Antreasyan *et al.*, Phys. Rev. Lett. 39, 906 (1977).

[11] J. W. Cronin *et al.*, Phys. Rev. D 11, 3105 (1975), and references contained therein; U. Becker *et al.*, Phys. Rev. Lett. 37, 1731 (1977); L. Kluberg *et al.*, Phys. Rev. Lett. 38, 670 (1977).

[12] See, for example, Refs. 4–12 of Kluberg *et al.*, Ref. 10.

[13] Yu. M. Antipov *et al.*, Phys. Lett. 76B, 235 (1978).

[14] C. B. Newman *et al.*, second following Letter [Phys. Rev. Lett. 42, 951 (1979)].